# INVESTIGATING THE VERTICAL STRUCTURE OF UPDRAFT HELICITY IN AN IDEALIZED SUPERCELL SIMULATION

Jeffrey M. Milne[1,2,3]*, Israel L. Jirak [3], and Harold E. Brooks[4]

[1] *Cooperative Institute for Mesoscale Meteorological Studies*
[2] *University of Oklahoma, School of Meteorology*
[3] *NOAA/NWS/NCEP Storm Prediction Center*
[4] *NOAA/OAR National Severe Storms Laboratory*

## 1. INTRODUCTION

As numerical weather prediction models have become able to explicitly resolve convection, storm attribute diagnostics have been developed to forecast for severe weather. Updraft helicity (UH) is one such parameter to identify rotating updrafts (Kain et al. 2008). UH is defined as

$$UH = \int_{z_1}^{z_2} w\zeta dz \qquad (1)$$

where $w$ is the vertical velocity and $\zeta$ is the vertical vorticity, integrated over a vertical layer between $z_1$ and $z_2$. UH essentially reduces the three-dimensional wind field to a single number. This makes UH useful to forecasters, but at the potential cost of losing some information contained in the three dimensional wind field.

The layer over which UH is calculated is commonly 2-5km AGL to diagnose mid-level rotation and 0-3km to diagnose low-level rotation (Sobash et al. 2011, 2016). The 2-5km AGL layer was chosen "since the primary interest is on storm rotation in the lower to middle troposphere" (Kain et al. 2008).

When used as a surrogate for severe storm reports, 2-5km UH has shown utility in forecasting all types of severe weather (tornadoes, strong winds, and large hail; Sobash et al. 2011). Filtering 2-5km UH using environmental parameters has also shown utility in forecasting tornadoes (Gallo et al. 2016). Low level UH (0-3km) without environmental information has also shown skill in forecasting tornadoes (Sobash et al. 2016).

All current methods of calculating UH use a fixed layer in the calculation, but Milne et al. (2018) found that $w\zeta$ often extends beyond the typical 2-5km (or 0-3km) AGL layer typically used in calculating UH. There were also considerable variations in the vertical distribution of $w\zeta$ from storm to storm and from day to day. Additionally, some simulated storms had

---
*Corresponding author address:* 120 David L. Boren Blvd, Ste 2600, Norman, OK 73072;
E-mail: jeffrey.milne@noaa.gov.

| Model Version | v3.4.1 |
|---|---|
| Grid spacing | 3km |
| Vertical levels | 41 |
| Time step | 12s |
| Boundary layer | none |
| Microphysics | WSM6 |

TABLE 1. WRF model configuration

areas of negative $w\zeta$ within an updraft within the 2-5km layer.

This study proposes a new method of calculating UH and discusses the differences between the new proposed method and the current method in two idealized cases.

## 2. DATA AND METHODS

### 2.1. Model details

An idealized 3-dimensional WRF simulation (configuration summarized in Table 1) was performed to demonstrate a new method of UH calculation. For the supercell simulations, the domain was 105x105 grid squares, and the simulation ran for 5 hours. For the squall line simulations, the domain was 210x210 grid squares, and the simulation ran for 10 hours. The full 3-dimensional wind field was output every 5 minutes to allow for instantaneous calculations of $w$ and $\zeta$ every 5 minutes. The model-calculated hourly maximum 2-5km UH was also output every hour.

There were two soundings used, one to simulate a supercell (Figure 1) and one to simulate a squall line (Figure 2). The supercell sounding and hodograph are the default found in WRF for simulating a supercell. The squall line sounding is the same as the supercell sounding, while the squall line hodograph was based on Weisman and Klemp (1984).

### 2.2. New UH calculation

Milne et al. (2018) found that positive $w\zeta$ existed outside of the typical 2-5km layer used in the cal-
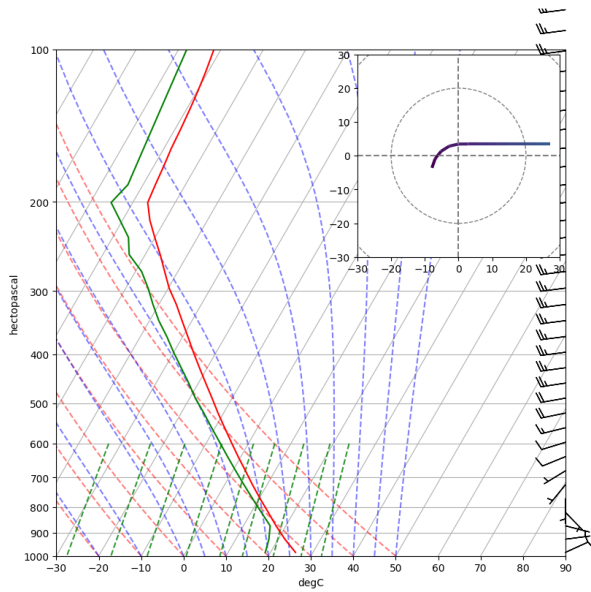
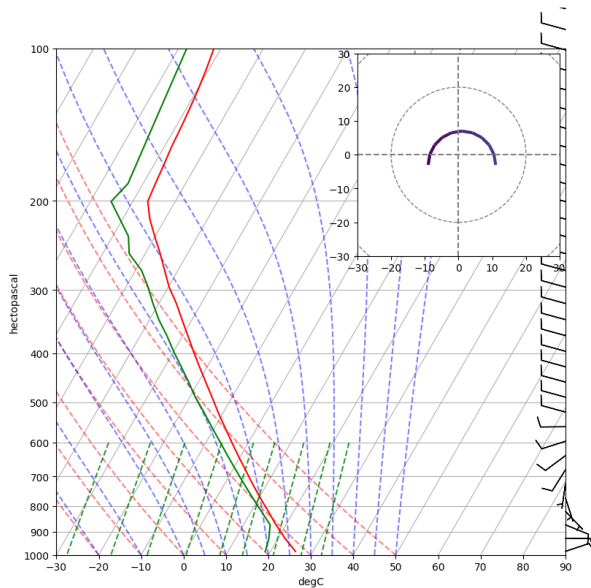**FIG. 1.** Sounding and hodograph used to generate a simulated supercell.



**FIG. 2.** Sounding and hodograph used to generate a simulated squall line.

culation of UH. A new calculation of UH was formulated to scale with the storm and not include downdrafts. Additionally, separate maximum and minimum fields were desired since hourly minimum UH can also be a useful forecasting parameter (Wendt et al. 2016). Therefore, the new UH calculation integrates from the surface to the lowest level of downward $w$. The calculation is done separately for $\zeta > 0$ (to create an hourly maximum field) and for $\zeta < 0$ (to create an hourly minimum field). In a mathematical sense,

$$UH_{new} = \int_0^{z_{w<0}} w\zeta dz. \tag{2}$$

The height at which the calculation stops is also output as part of the calculation and it may provide additional utility in forecasting.

Calculation of the new UH was done in postprocessing and yielded instantaneous fields every 5 minutes. These fields were aggregated over the entire simulation to create a simulation maximum. This was compared with the aggregated hourly maximum UH field output by the model.

## 3. RESULTS

### 3.1. Supercell

The supercell simulation ran on a 105x105 grid square (315kmx315km) domain for 5 hours. In that period, a right-moving supercell forms and grows upscale into a quasi-linear convective system. The simulation ends as the storm leaves the domain. A snapshot of the simulated reflectivity is shown in Figure 3.

An analysis similar to Milne et al. (2018) was done on the supercell simulation to confirm that the vertical distribution of $w\zeta$ was substantially similar to what was seen in the earlier study. The time-height cross section of $w\zeta$ in the idealized supercell (Figure 4) is similar to those found in Milne et al. (2018). Namely, both positive and negative $w\zeta$ exist throughout the atmospheric column. In fact, positive $w\zeta$ is maximized above 5km.

The simulation maximum of new UH (Figure 6) and current UH (Figure 5) show some key differences between the two calculations. In the new calculation, there is a strong positive signature to the left of the supercell's motion. This feature is only faintly visible on the current calculation. On the simulated reflectivity field, this feature is visible and initially appeared to be an anticyclonically rotating left-moving supercell. The new UH calculation,
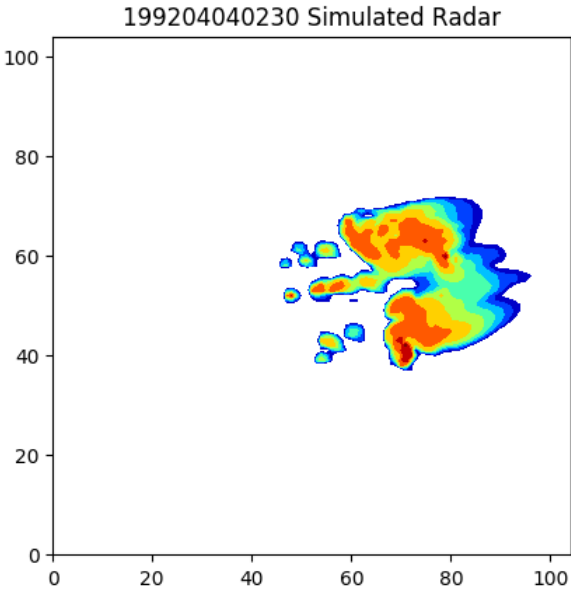
**Fɪɢ. 3.** Simulated reflectivity 1km above the ground, 2.5 hours into the supercell simulation. The supercell can be seen at the southern edge of the reflectivity.
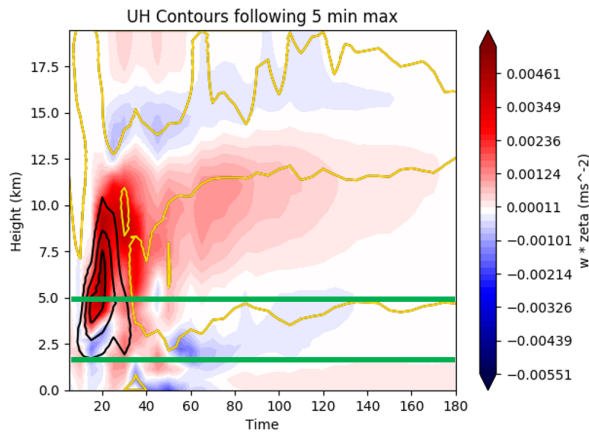


**Fɪɢ. 4.** Time-height cross section of $w\zeta$ for the idealized supercell, following Milne et al. (2018). Areas of positive $w\zeta$ are shaded in red, while areas of negative $w\zeta$ are shaded in blue. Solid black contours are upward vertical velocity every 5ms$^{-1}$. The gold contour is the line of $w = 0$. The green lines highlight the 2-5km layer typically used to calculate UH.
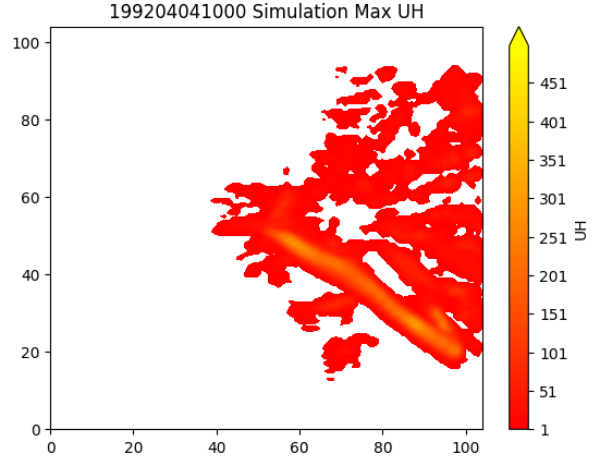


**Fɪɢ. 5.** Simulation maximum of UH as output by the model.

suggests that the simulated storm is cyclonically rotating, and ingests the outflow from the more dominant right-moving supercell.

In the current UH calculation, the path of the right-moving supercell is highlighted as a maximum in UH. In the new UH calculation however, there is a relative minimum along the same path. The simulation minimum of the new UH calculation (Figure 7) is minimized in the same place as in Figure 6. This suggests that the simulated supercell is initially dominated by a cyclonically rotating updraft, which then weakens. The storm is then dominated by an anticyclonically rotating updraft, which again weakens before a cyclonically rotating updraft dominates for the remainder of the simulated storm's life.

There is another relative minimum in Figure 7 in the northeast part of the domain, which could indicated that an anticyclonically rotating updraft developed as the storm was transitioning to a quasi-linear convective system.

### 3.2. Squall line

The squall line simulation ran on a 210x210 grid square (630kmx630km) domain. A right-moving supercell forms and quickly grows upscale into a squall line. There are some embedded cells in the line. A snapshot of radar reflectivity in the simulated storm is shown in Figure 8. As in the supercell case, the simulation ends as the line leaves the domain.

As in the supercell case, there are some key differences between the simulation maxima of the current UH calculation (Figure 9) and the new UH cal-
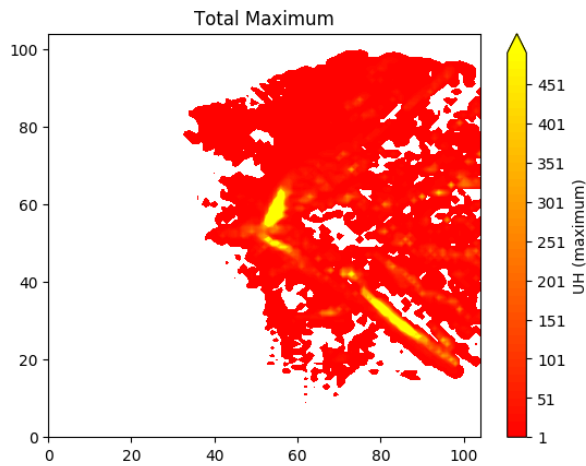
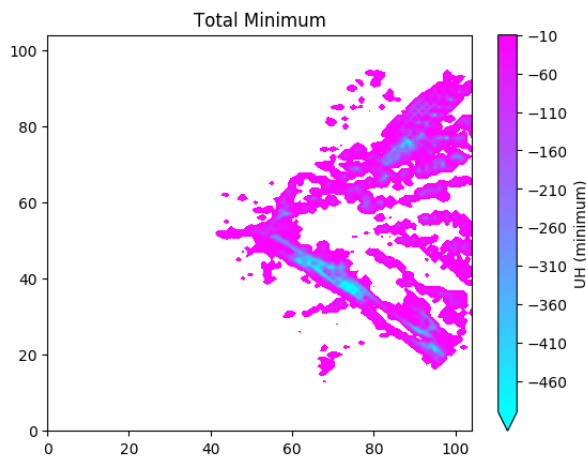**FIG. 6.** Simulation maximum of the new UH calculation for the idealized supercell.



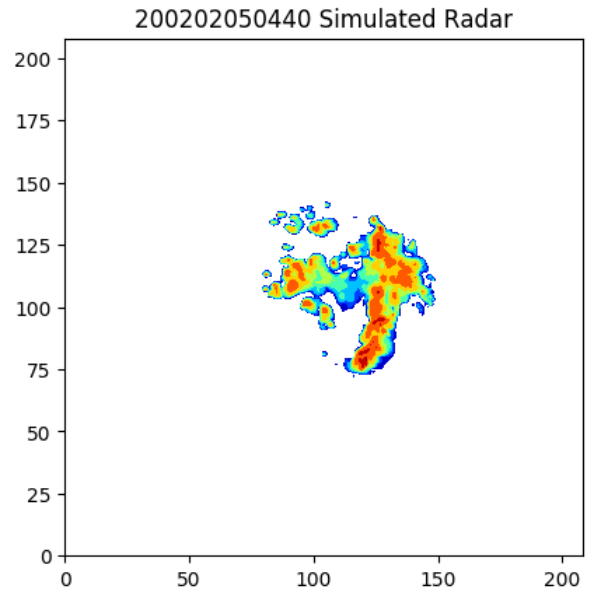**FIG. 7.** As in Figure 6, but the simulation minimum.



**FIG. 8.** As in Figure 3 for 4 hours and 40 minutes into the squall line simulation.

culation (Figure 10). While the track of the initial right-moving supercell is apparent in the current UH calculation, the new calculation only highlights the initial portion of the track.

In the minimum of the new UH calculation (Figure 11), the track highlighted in the current UH calculation is also highlighted as a minimum. This indicates similar behavior to the supercell case. The storm is initially dominated by a cyclonically rotating updraft, which weakens and an anticyclonically rotating updraft strengthens. The difference is that in the squall line case, the storm dissipates before a cyclonically rotating updraft can take over again. This cyclonic-anticyclonic alternation has not been documented before, and more research will need to be done to determine what that signal means.

## 4. CONCLUSIONS AND FUTURE WORK

The proposed new UH calculation captures more information than the current calculation. Namely, the new calculation can give information about rotation throughout the column rather than just the fixed layer in the current UH calculation. The new UH calculation can also provide information about the depth of the simulated storm, though more research is needed to fully explore the data.

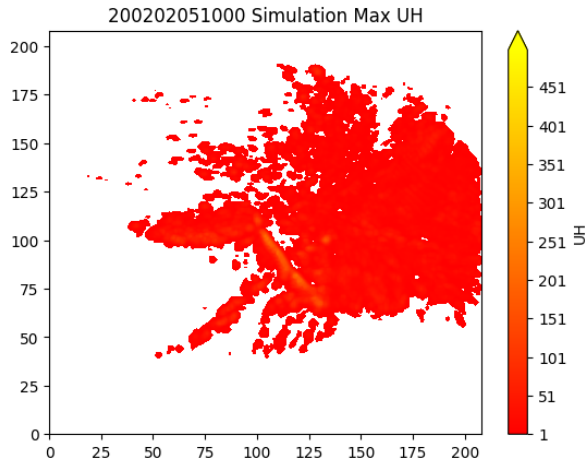The new UH calculations presented here were also done entirely in post processing, which

4

**FIG. 9.** As in Figure 5 for the squall line case.
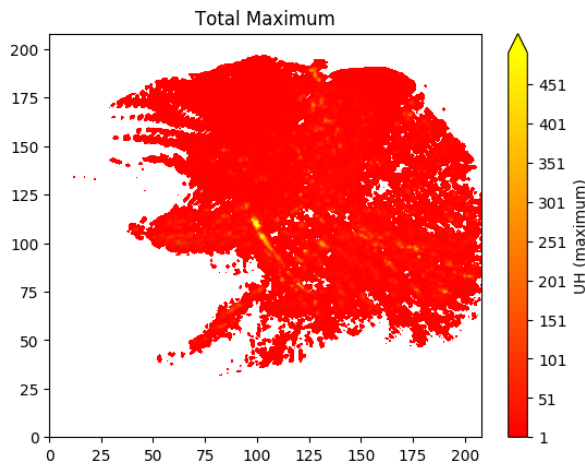


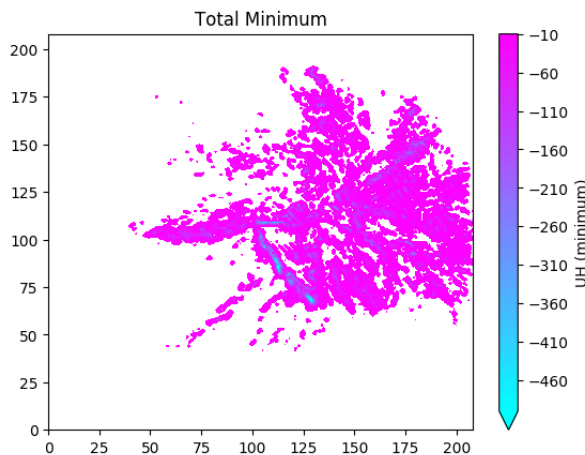**FIG. 10.** As in Figure 6 for the squall line case.



**FIG. 11.** As in Figure 7 for the squall line case.

presents a hurdle to implementing the new UH calculation in real-world simulations. Work is ongoing on writing the new calculation in Fortran.

Once the calculation is implemented within the model, more extensive comparisons can be done on real world cases between the new and current UH calculations. These comparisons will include qualitative comparisons as presented here and quantitative evaluations of forecasts made using the new UH calculation.

**REFERENCES**

Gallo, B. T., A. J. Clark, and S. R. Dembek, 2016: Forecasting Tornadoes Using Convection-Permitting Ensembles. *Weather and Forecasting*, **31 (1)**, 273–295, doi:10.1175/WAF-D-15-0134.1, URL http://journals.ametsoc.org/doi/10.1175/WAF-D-15-0134.1.

Kain, J. S., and Coauthors, 2008: Some Practical Considerations Regarding Horizontal Resolution in the First Generation of Operational Convection-Allowing NWP. *Weather and Forecasting*, **23 (5)**, 931–952, URL http://journals.ametsoc.org/doi/abs/10.1175/WAF2007106.1.

Milne, J. M., I. L. Jirak, and H. E. Brooks, 2018: Investigating the Vertical Structure of Updraft Helicity in Convection-Allowing Models. *29th Conference on Severe and Local Storms*, Stowe, VT, URL https://ams.confex.com/ams/29SLS/webprogram/Paper348472.html.

Sobash, R. A., J. S. Kain, D. R. Bright, A. R. Dean, M. C. Coniglio, and S. J. Weiss, 2011: Probabilistic Forecast Guidance for Severe Thunderstorms Based on the Identification of Extreme Phenomena in Convection-

Allowing Model Forecasts. *Weather and Forecasting*, **26 (5)**, 714–728, doi:10.1175/WAF-D-10-05046.1, URL http://journals.ametsoc.org/doi/abs/10.1175/WAF-D-10-05046.1.

Sobash, R. A., G. S. Romine, C. S. Schwartz, D. J. Gagne, and M. L. Weisman, 2016: Explicit Forecasts of Low-Level Rotation from Convection-Allowing Models for Next-Day Tornado Prediction. *Weather and Forecasting*, **31 (5)**, 1591–1614, doi:10.1175/WAF-D-16-0073.1, URL http://journals.ametsoc.org/doi/10.1175/WAF-D-16-0073.1.

Weisman, M. L., and J. B. Klemp, 1984: The structure and classification of numerically simulated convective storms in directionally varying wind shears. *Monthly Weather Review*, **112 (12)**, 2479–2498, doi:10.1175/1520-0493(1984)112<2479:TSACON>2.0.CO;2.

Wendt, N. A., I. L. Jirak, and C. J. Melick, 2016: Verification of Severe Weather Proxies from the NSSL-WRF for Hail Forecasting. *28th Conference on Severe and Local Storms*, Portland, OR, URL https://ams.confex.com/ams/28SLS/webprogram/Paper300913.html.